Supplementary information

Spatiotemporal Programming of Photosensitizer Relocalization for Nucleolus-Directed Pyroptosis

Zhuoran Xia[a,b], Tianping Xia[a], Jie Fei[a], Mingwang Yang[a], Xueze Zhao[a*], Wen Sun[a], Jianjun Du[a], Dayong Jin[c], Xiaojun, Peng[a], Jiangli Fan[a,b*]

[a] State Key Laboratory of Fine Chemicals, Frontiers Science Center for Smart Materials Oriented Chemical Engineering, Dalian University of Technology, Dalian 116024, P. R. China

[b] Ningbo Institute of Dalian University of Technology, Ningbo 315016, P. R. China

[c] Institute for Biomedical Materials & Devices, Faculty of Science, University of Technology Sydney, Ultimo, New South Wales 2007, Australia

* Corresponding author: Xueze Zhao & Jiangli Fan.

Email: zhaoxz@dlut.edu.cn; fanjl@dlut.edu.cn.

Table of Contents

1. Experimental section

Materials

Reagents and chemicals used in the synthesis of final products and intermediate were purchased from Energy-Chemical, Bide Pharmatech Ltd and Aladdin Biochemical Technology Ltd without further purification. The reactive oxygen species (ROS) detection reagents (DPBF: 1,3-diphenylisobenzofuran; DCFH-DA: 2,7-Dichlorodihydrofluorescein diacetate; DHE: dihydroethidium; ABDA: 9,10-Anthracenediyl-bis (methylene) dimalonic acid) were purchased from Beyotime Biotech Inc. and Sigma-Aldrich. Mito Tracker Deep Red^{FM} (MTDR), Mito Tracker Green^{FM} (MTG), 4',6-diamidino-2-phenylindole (DAPI) and Hoechst 33342 were purchased from Life Technologies Co. (USA). Calcein-AM/propidium iodide (PI) cell viability assay kit, mitochondrial membrane potential assay kit with JC-1, mitochondrial permeability transition pore assay kit, adenosine 5'-triphosphate (ATP) and lactate dehydrogenase (LDH) assay kit were purchased from Beyotime Biotech Inc. CT DNA (deoxyribonucleic acid from calf thymus, dsDNA) and yeast RNA (ribonucleic acid from torula yeast, ssRNA) were purchased from Solarbio® life science. DNase and RNase were purchased from Solarbio® life science. Phosphate buffer saline (PBS, pH = 7.4, 10.0 mmol/L), Dulbecco's modified eagle medium (DMEM) and trypsin-EDTA solution (0.25%, without phenol red) were purchased from Solarbio® life science. 3-(4,5-dimethylthiazol-2-yl)2,5-diphenyltetrazolium bromide (MTT) was purchased from Shanghai Titan Scientific Co., Ltd. (Shanghai, China). Calreticulin (CRT) rabbit polyclonal antibody and high mobility group box 1 (HMGB1) rabbit polyclonal antibody were purchased from Proteintech Group Inc. NLRP3 monoclonal antibody and p53 monoclonal antibody were purchased from Thermo Fisher Scientific. Protein IL-6, IFN-γ, IL-1β and IL-18 ELISA Kit were purchased from Shanghai Enzyme-linked Biotechnology Co., Ltd. APC Anti-Mouse CD3 Antibody [17A2], FITC Anti-Mouse CD4 Antibody [GK1.5], PE Anti-Mouse CD8a Antibody [53-6.7], FITC Anti-Mouse CD11c Antibody [N418], APC

Anti-Mouse CD80 Antibody [16-10A1], PE Anti-Mouse CD86 Antibody [GL-1] were purchased from Elabscience Biotechnology Co., Ltd. For solution and in vitro tests, stock solution of compounds (N1–N9) in DMSO (10 mM) was prepared. NMR spectra were detected by Bruker Avance III 400 and 500 spectrometer. Mass spectrometric (ESI-MS) data were obtained with LTQ Orbit rap XL instruments.

Cell culture and cell cytotoxicity assay

MCF-7, HepG2, and 4T1 cells were selected for all cell experiments, and all kinds of cell lines were purchased from the Institute of Basic Medical Sciences of the Chinese Academy of Medical Sciences. Cells, which were cultured in Dulbecco's modified Eagle's medium (DMEM, Invitrogen) supplemented with 10% fetal bovine serum (PAN-Biotech GmbH), were seeded in 25 cm^2 culture flask at 37 ºC under a mixture of 5% CO_2 and 95% air atmosphere. For cell cytotoxicity assay, 4T1, HepG2 and MCF-7 cells were seeded at a density of 1×10^5 cells per well in a 96-well plate and cultured for 24 h. The cells were then incubated with increasing concentration of N1–N9. After 24 h, the media were replaced with MTT (0.5 mg/mL) reagent in cell culture medium and incubated for another 4 h at 37 °C. After pouring out the culture medium, 100 μL of DMSO was added into each well. Absorbance was measured at 490 nm. The photocytotoxicity assay of N7–N9 followed a procedure similar to that described above, using 520-540 nm monochromatic light as the light source.

Intracellular ROS detection

The ROS generation inside the cells upon light irradiation was detected by DCFH-DA (a ROS scavenger), SOSG (a $^1O_2$ scavenger), DHE (a $O_2\bullet^-$ scavenger). 4T1 cells were incubated in 25 cm^2 culture flask at 37 ºC under a mixture of 5% CO_2 and 95% air atmosphere. After adding DCFH-DA, SOSG or DHE (10 μM) and N7–N9 (2 μM) for 10 min, 4T1 cells were irradiated with 520 nm monochromatic light (20 mW/cm^2, 10 min). Confocal fluorescence images were collected using the following parameters. Excitation wavelength for DCFH-DA, SOSG: 488 nm, emission collection: 500-540 nm; Excitation wavelength for DHE: 561 nm, emission collection: 570-600 nm.

Measurement of cellular CRT, HMGB-1, p53 and NLRP3

To conduct immunofluorescence staining for CRT expose and HMGB-1 release, 4T1 cells (~10^5 cells) were incubated in petri dishes at 37 °C under 5 wt %/vol CO_2 for 24 h. Subsequently, 4T1 cells in petri dishes were divided into four groups: G1: control; G2: N7 (2 μM); G3: light (20 mW/cm^2, 10 min) G4: N7 (2 μM) + light (520 nm, 20 mW/cm^2, 10 min). Following this, four groups were treated within 30 min. Then, cells were washed with PBS buffer and fixed using 1% paraformaldehyde at room temperature for 30 min. Fixed cells were blocked with 1% BSA for 30 min and then incubated overnight at 4 °C with a 1:1000 dilution of either CRT or HMGB-1 primary antibody in block buffer. On the following day, cells were washed 3 times with PBS buffer and incubated with Alexa Fluor 647-conjugated secondary antibody at room temperature for 3 h. Subsequently, nuclear DNA was stained with DAPI, and fluorescent imaging were acquired using confocal laser scanning microscopy.

Establishment of tumor-bearing mice models

Female Balc/c mice (4-5 week) were purchase from the SPF laboratory animal center at Dalian Medical University with the permission number of SCXK 2003-0003. The tumor implants were established by sub-skin injection of 1×10^6 4T1 cells suspended in 100 μL of PBS buffer. Experiments with tumor-bearing mice were performed about 7-10 days, when implants grew up to about 150 mm^3 in size. Tumor size was estimated as follows: V = length × width × height.

Fluorescent imaging of 4T1 tumor-bearing BALB/c mice

4T1 cells were subcutaneously injected into the mice to establish tumor-bearing model. When tumor volumes reached ~ 150 mm, N7 (4 μM, 100 μL) was administered to mice via peritumoral injection into the tumor site, and fluorescence imaging was performed before and after the injection.

***In vivo* photo dynamic therapy (PDT) of tumor-bearing mice**

For the evaluation of the *in vivo* PDT effect and immune activation capacity of **N7**, tumor-bearing mice were randomized into four groups: G1: control; G2: **N7** (4 μM,

100 μL); G3: light (30 mW/cm^2, 15 min) G4: **N7** (4 μM, 100 μL) + light (520 nm, 30 mW/cm^2, 15 min) and each consisted of eight mice. Tumor volumes were measured using a vernier caliper throughout the treatment period. For the G2 and G4 experimental groups, N7 was administered via peritumoral injection. 20 min later, the G3 and G4 groups were subjected to irradiation. Afterward, tumor size and weight of mice were monitored every two days for 14 days. 7 days post-treatment, four mice from each group were randomly selected and euthanized to collect tumor tissues and spleens. Subsequently, relevant immune cells ($CD3^+CD4^+$ T cells, $CD3^+CD8^+$ T cells and $CD11_c^+CD80^+CD86^+$ DCs) and cytokines (IL-6, IL-18, IL-1β and IFN-γ) were isolated. Immune cell populations were analyzed by flow cytometry, while the procedures for immune cell extraction and cytokine testing were performed according to previously reported method[1,2].

1. Synthetic methods

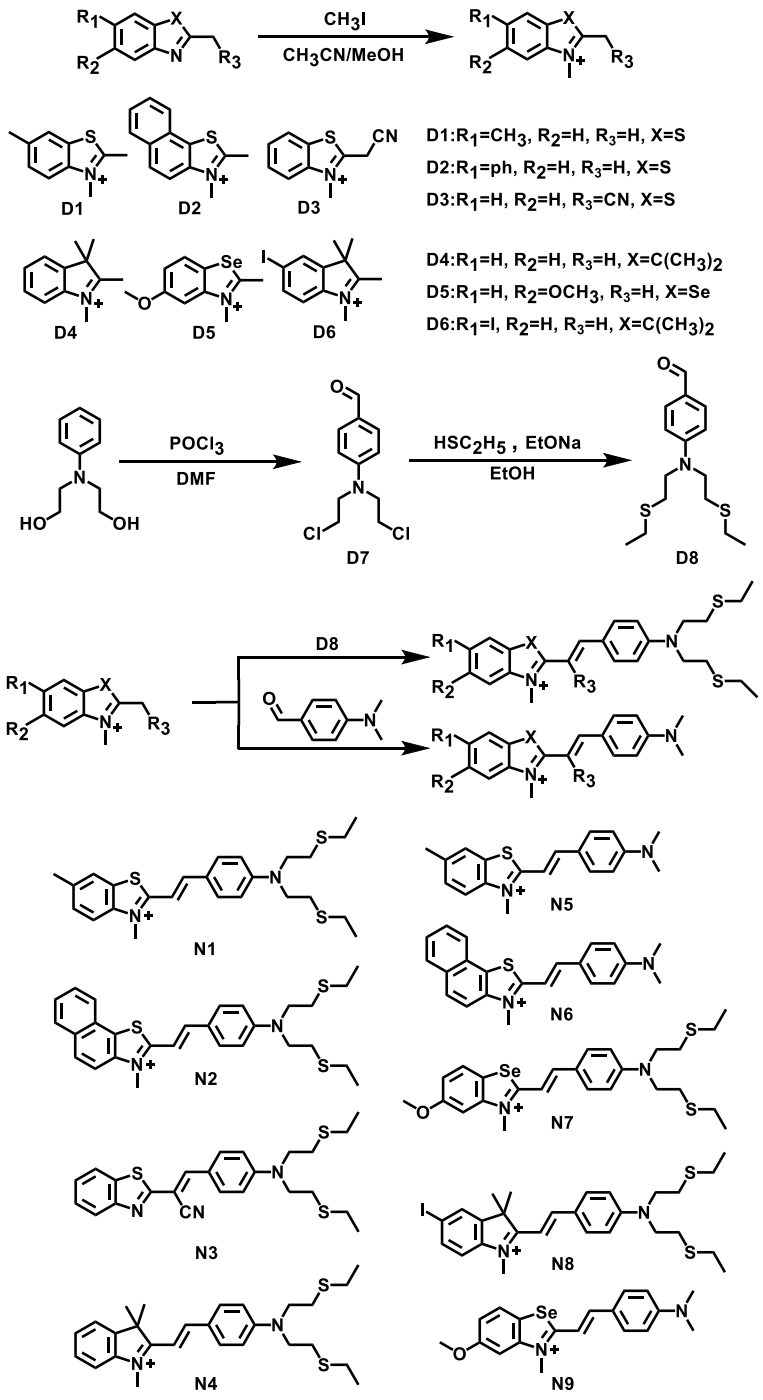

Scheme S1. Synthetic route of probe **N1-N7**.

Synthetic of compound D1-D8

Synthetic intermediate **D1-D8** were synthesized according to previously reported literature procedures[3-5].

Synthetic of compound N1-N9

Synthetic intermediate **N1-N9** were synthesized based on known procedure[3].

N1

^{1}H NMR (400 MHz, DMSO-d_6) δ 8.11 (s, 1H), 8.07 – 7.97 (m, 2H), 7.90 (d, J = 8.9 Hz, 2H), 7.68 – 7.57 (m, 2H), 6.83 (d, J = 9.0 Hz, 2H), 4.22 (s, 3H), 3.73 – 3.63 (m, 4H), 2.79 – 2.70 (m, 4H), 2.63 (q, J = 7.4 Hz, 4H), 1.22 (t, J = 7.4 Hz, 8H).

^{13}C NMR (101 MHz, DMSO-d_6) δ 170.99, 151.34, 149.69, 140.57, 138.42, 133.30, 130.61, 127.45, 123.77, 122.47, 116.18, 112.33, 107.44, 50.96, 36.13, 28.51, 25.64, 21.41, 15.36.

TOF MS: m/z calcd for $C_{25}H_{33}N_2S_3^+$: 451.1800, found: 451.1797.

N2

^{1}H NMR (400 MHz, DMSO-d_6) δ 8.35 (d, J = 9.2 Hz, 1H), 8.23 (dd, J = 13.8, 8.6 Hz, 3H), 8.12 (d, J = 15.3 Hz, 1H), 7.91 (d, J = 8.8 Hz, 2H), 7.86 (d, J = 7.5 Hz, 1H), 7.79 (t, J = 7.5 Hz, 1H), 7.71 (d, J = 15.4 Hz, 1H), 6.83 (d, J = 8.8 Hz, 2H), 4.35 (s, 3H), 3.74 – 3.61 (m, 4H), 2.81 – 2.71 (m, 4H), 2.63 (q, J = 7.4 Hz, 4H), 1.22 (t, J = 7.3 Hz, 6H).

^{13}C NMR (101 MHz, DMSO-d_6) δ 169.99, 151.35, 149.42, 140.91, 133.26, 131.53, 130.94, 129.93, 129.72, 128.66, 124.13, 122.52, 114.69, 112.39, 107.46, 50.98, 36.67, 28.51, 25.64, 15.37.

TOF MS： m/z calcd for $C_{28}H_{33}N_2S_3^+$: 493.1800, found: 493.1791.

N3

^{1}H NMR (600 MHz, Chloroform-d) δ 8.24 (s, 1H), 8.07 (d, J = 8.2 Hz, 1H), 8.01 (d, J = 8.7 Hz, 2H), 7.88 (d, J = 7.9 Hz, 1H), 7.51 (ddd, J = 8.3, 7.2, 1.2 Hz, 1H), 7.45 – 7.36 (m, 1H), 6.73 (d, J = 8.8 Hz, 2H), 3.66 (t, J = 7.7 Hz, 4H), 2.80 – 2.75 (m, 4H), 2.63 (q, J = 7.3 Hz, 4H), 1.31 (s, 6H).

^{13}C NMR (101 MHz, DMSO-d_6) δ 160.09, 145.54, 142.41, 128.93, 122.13, 120.66, 117.85, 116.83, 116.15, 113.21, 106.94, 46.76, 24.14, 21.76, 10.21.

TOF MS：m/z calcd for $C_{24}H_{28}N_3S_3^+$: 454.1440, found: 454.1443.

N4

^{1}H NMR (400 MHz, DMSO-d_6) δ 8.31 (d, J = 15.8 Hz, 1H), 8.09 (d, J = 8.7 Hz, 2H), 7.83 – 7.76 (m, 1H), 7.73 (d, J = 7.9 Hz, 1H), 7.61 – 7.52 (m, 1H), 7.50 (t, J = 7.4 Hz, 1H), 7.30 (d, J = 15.8 Hz, 1H), 6.89 (d, J = 8.8 Hz, 2H), 3.99 (s, 3H), 3.74 (t, J = 7.5 Hz, 4H), 2.78 (t, J = 7.5 Hz, 4H), 2.64 (q, J = 7.4 Hz, 4H), 1.76 (s, 6H), 1.22 (t, J = 7.4 Hz, 6H).

^{13}C NMR (101 MHz, DMSO-d_6) δ 180.37, 154.29, 152.56, 143.15, 142.52, 129.20, 128.23, 123.24, 123.13, 114.24, 112.62, 106.34, 51.48, 50.98, 33.67, 28.51, 26.60, 25.63, 15.34.

TOF MS：m/z calcd for $C_{27}H_{37}N_3S_3^+$: 453.2393, found: 453.2378.

N5

^{1}H NMR (400 MHz, DMSO-d_6) δ 8.09 (s, 1H), 8.03 (d, J = 17.5 Hz, 2H), 7.90 (d, J = 8.5 Hz, 2H), 7.61 (d, J = 12.1 Hz, 2H), 6.89 – 6.78 (m, 2H), 4.21 (s, 3H), 3.10 (s, 6H), 1.23 (s, 3H).

^{13}C NMR (101 MHz, DMSO-d_6) δ 170.95, 150.06, 140.55, 138.29, 133.12, 130.53, 123.76, 116.09, 112.41, 106.86, 36.04, 21.40.

TOF MS：m/z calcd for $C_{19}H_{21}N_2S^+$: 309.1420, found: 309.1415.

N6

^{1}H NMR (400 MHz, DMSO-d_6) δ 8.34 (d, J = 9.1 Hz, 1H), 8.24 (d, J = 8.1 Hz, 1H), 8.19 (dd, J = 8.7, 6.7 Hz, 2H), 8.10 (d, J = 15.3 Hz, 1H), 7.92 – 7.83 (m, 3H), 7.78 (ddd, J = 8.2, 7.0, 1.3 Hz, 1H), 7.68 (d, J = 15.3 Hz, 1H), 6.80 (d, J = 8.7 Hz, 2H), 4.34 (s, 3H), 3.07 (s, 6H).

^{13}C NMR (101 MHz, DMSO-d_6) δ 169.93, 153.80, 149.79, 140.85, 133.07, 131.48, 130.85, 129.91, 129.68, 128.57, 126.39, 124.58, 124.09, 121.98, 114.64, 112.42, 106.83, 36.58.

TOF MS：m/z calcd for $C_{22}H_{21}N_2S^+$: 345.1420, found: 345.1413.

N7

^{1}H NMR (400 MHz, CD_2Cl_2-d_2) δ 8.35 (d, *J* = 8.9 Hz, 1H), 7.86 – 7.74 (m, 3H), 7.43 (d, *J* = 15.0 Hz, 1H), 7.14 (d, *J* = 2.4 Hz, 1H), 7.07 (dd, *J* = 8.9, 2.4 Hz, 1H), 6.71 (d, *J* = 8.8 Hz, 2H), 4.21 (s, 3H), 3.93 (s, 3H), 3.69 – 3.62 (m, 4H), 2.81 – 2.73 (m, 4H), 2.63 (q, *J* = 7.4 Hz, 4H), 1.29 (t, *J* = 7.4 Hz, 6H).

^{13}C NMR (101 MHz, CD_2Cl_2-d_2) δ 181.05, 162.21, 152.81, 145.70, 134.70, 129.46, 123.82, 120.66, 117.04, 113.46, 110.53, 102.21, 57.62, 52.90, 39.22, 30.18, 27.70, 16.14.

TOF MS：m/z calcd for $C_{25}H_{33}N_2OS_2Se^+$: 521.1194, found: 521.1194.

N8

^{1}H NMR (400 MHz, DMSO-d_6) δ 8.32 (d, J = 15.7 Hz, 1H), 8.26 – 8.19 (m, 1H), 8.08 (d, J = 8.6 Hz, 2H), 7.94 – 7.86 (m, 1H), 7.52 (d, J = 8.4 Hz, 1H), 7.24 (d, J = 15.6 Hz, 1H), 6.89 (d, J = 8.8 Hz, 2H), 3.93 (s, 3H), 3.74 (t, J = 7.4 Hz, 4H), 2.77 (t, J = 7.4 Hz, 4H), 2.63 (q, J = 7.4 Hz, 4H), 1.74 (s, 6H), 1.21 (t, J = 7.3 Hz, 6H).

^{13}C NMR (151 MHz, DMSO-d_6) δ 178.72, 153.70, 151.78, 144.23, 141.35, 136.70, 130.88, 122.29, 115.08, 111.67, 104.92, 92.59, 50.35, 49.92, 32.53, 27.44, 25.38, 24.56, 14.25.

TOF MS：m/z calcd for $C_{27}H_{36}N_2S_2I^+$: 579.1359, found: 579.1358.

N9

^{1}H NMR (400 MHz, DMSO-d_6) δ 8.19 (d, *J* = 8.9 Hz, 1H), 8.09 (d, *J* = 15.1 Hz, 1H), 7.92 (d, *J* = 8.7 Hz, 2H), 7.64 (d, *J* = 15.1 Hz, 1H), 7.57 (d, *J* = 2.4 Hz, 1H), 7.25 (dd, *J* = 8.9, 2.3 Hz, 1H), 6.84 (d, *J* = 8.8 Hz, 2H), 4.19 (s, 3H), 3.93 (s, 3H), 3.11 (s, 6H).

^{13}C NMR (101 MHz, DMSO-d_6) δ 180.67, 160.62, 153.93, 151.80, 145.06, 133.32, 127.86, 122.42, 119.60, 116.23, 112.46, 110.10, 102.28, 56.63, 37.30.

TOF MS：m/z calcd for $C_{19}H_{21}N_2OSe^+$: 373.0814, found: 373.0813.

2. Supplementary Figures

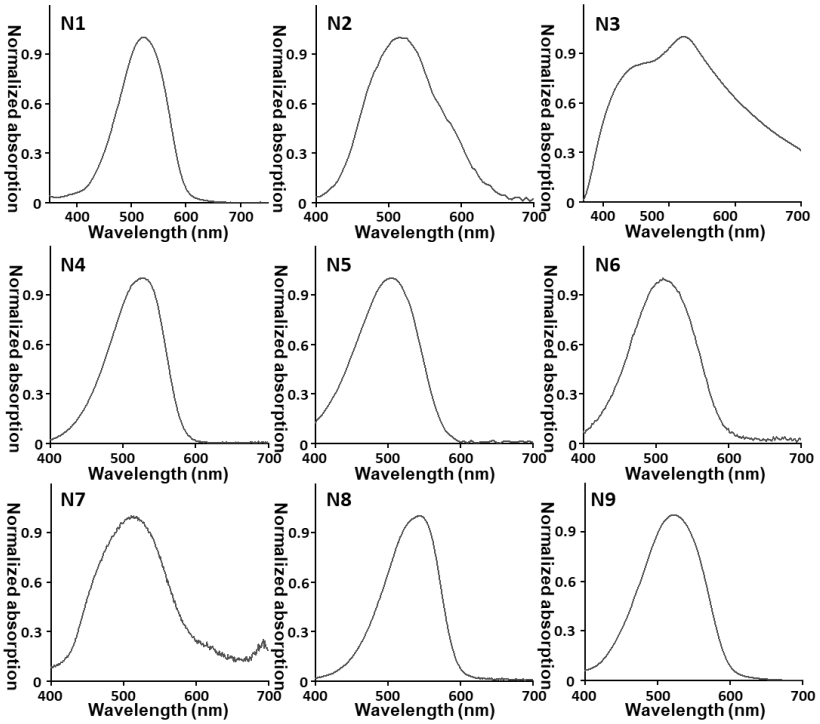

Supplementary Fig. 1 The absorbance spectra of N1-N9 in PBS solution.

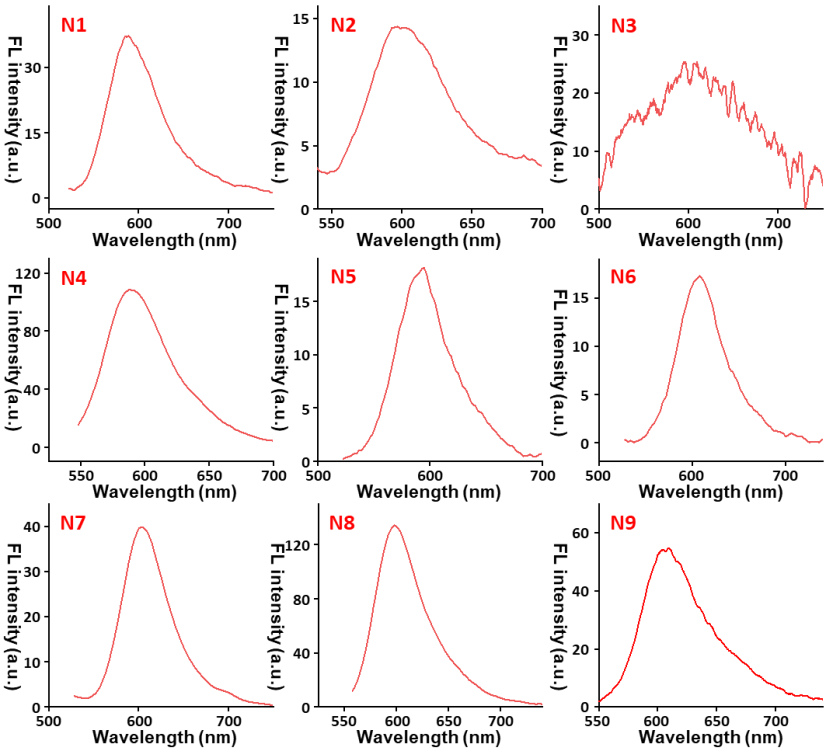

Supplementary Fig. 2 The emission spectra of N1–N9 in PBS solution.

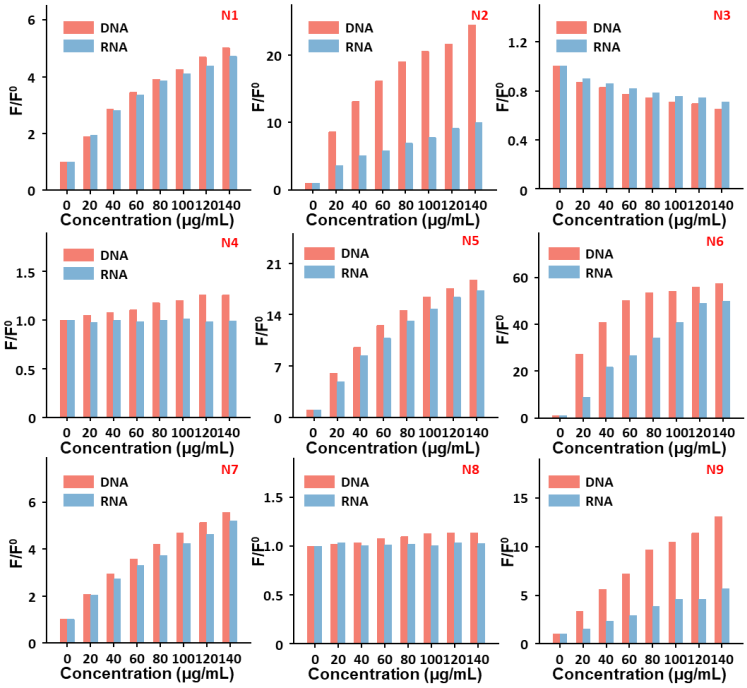

Supplementary Fig. 3 Fluorescence responses of N1–N9 (4 μM) to CT DNA (0-140 μg/mL) and yeast RNA (0-140 μg/mL) in PBS solution.

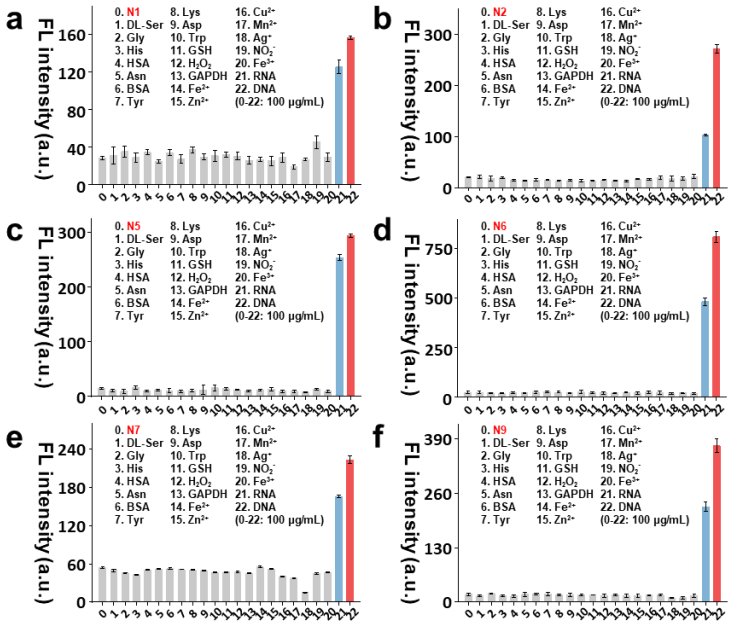

Supplementary Fig. 4 Fluorescence responses of N1 (a, 4 μM), N2 (b, 4 μM), N5 (c, 4 μM), N6 (d, 4 μM), N7 (e, 4 μM) and N9 (f, 4 μM) to yeast RNA (21: 20 μg/mL), CT DNA (22: 20 μg/mL) and other interferences in PBS solution (1. DL-Ser, 2. Gly, 3. His, 4. HSA, 5. Asn, 6. BSA, 7. Tyr, 8. Lys, 9. Asp, 10. Trp, 11. GSH, 12. H_2O_2, 13. GAPDH, 14. Fe^{2+}, 15. Zn^{2+}, 16. Cu^{2+}, 17. Mn^{2+}, 18. Ag^{+}, 19. NO_2^-, 20, Fe^{3+}, 100 μg/mL). HSA refers to human serum albumin and BSA refers to bovine serum albumin.

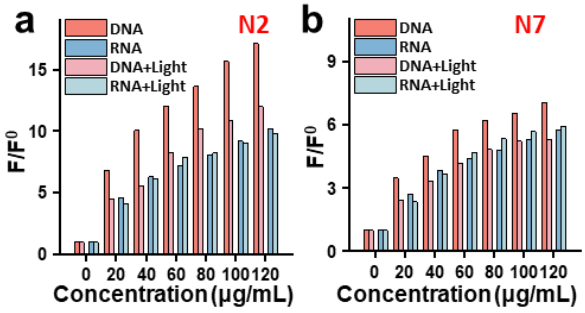

Supplementary Fig. 5 The fluorescence intensity ratio of N2 (a) and N7 (b) before and after binding to DNA (pUC18, 0-120 μg/mL) and RNA (SnoRD126, 0-120 μg/mL), nucleic acids were exposed to light illumination, 520 nm, 30 mW/cm^2, 10 min.

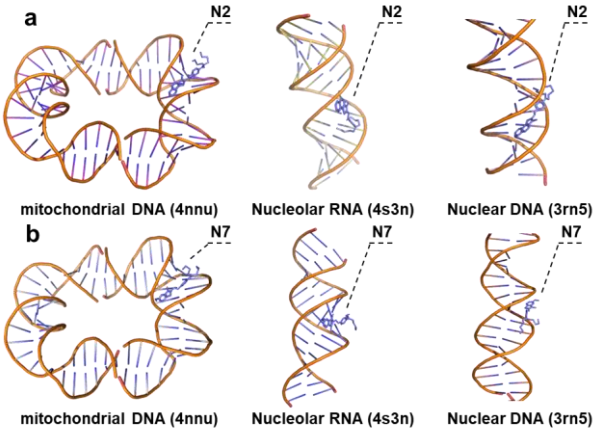

c

Compounds	4nnu	4s3n	3rn5
N2	-5.83	-4.18	-4.77
N7	-4.76	-4.56	-4.09

Supplementary Fig. 6 Molecular docking calculation of N2 (a) and N7 (b) with mitochondrial DNA (4nnu), nucleolar RNA (4s3n) and nuclear DNA (3rn5). (c) Calculated binding energy (kcal/mol) of N1, N2 and N7 in the presence of mitochondrial DNA (4nnu), nucleolar RNA (4s3n) and nuclear DNA (3rn5).

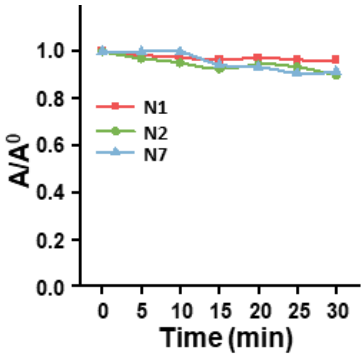

Supplementary Fig. 7 The ratio of the maximum absorbance to the initial absorbance of compounds (N1, N2 and N7) under continuous white light illumination.

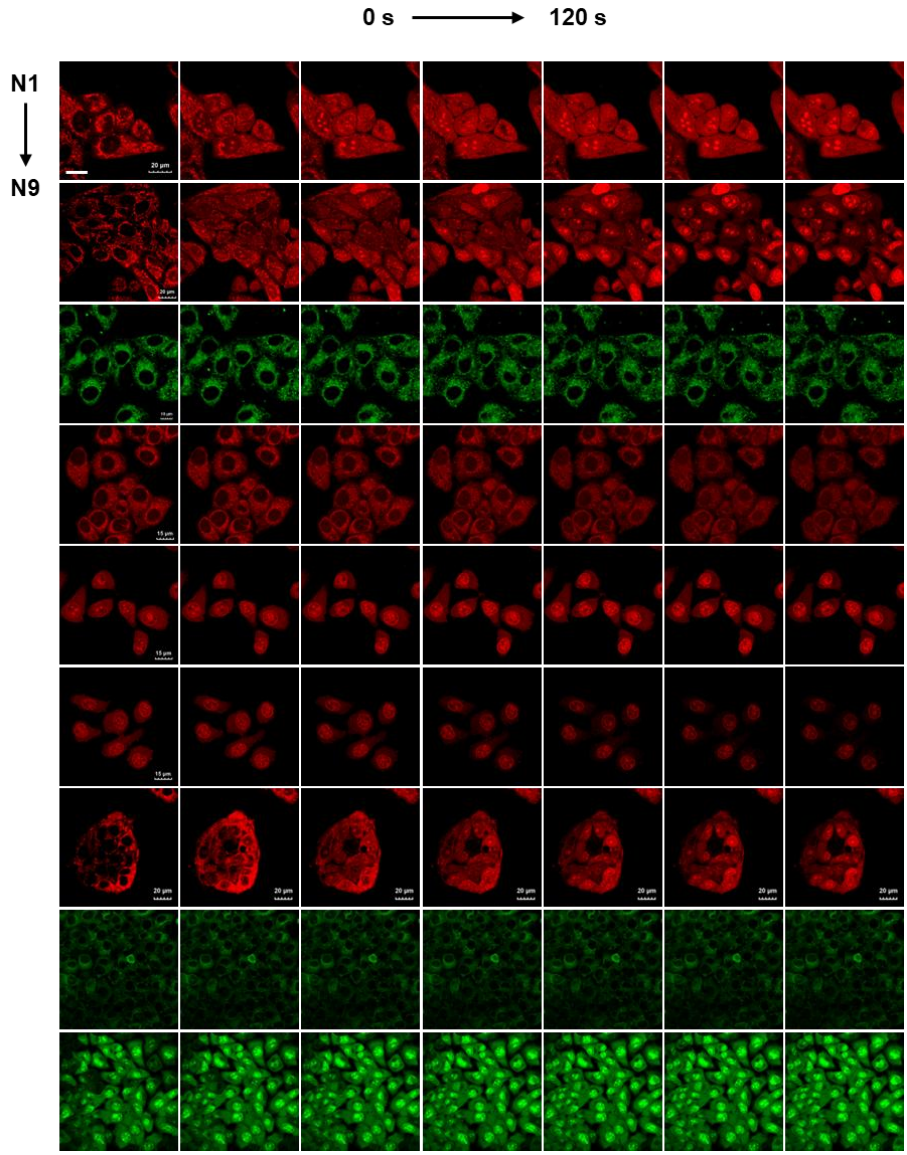

Supplementary Fig. 8 Fluorescent imaging of HepG2 cells stained with N1-N9 (2 μM) under light irradiation (collect images at 20 s intervals with continuous irradiation, the light is from the laser of confocal microscopy, 488 nm). N1-N9: λ_{ex} = 488 nm, λ_{em} = 600–650 nm. Scale bar: 20 μm.

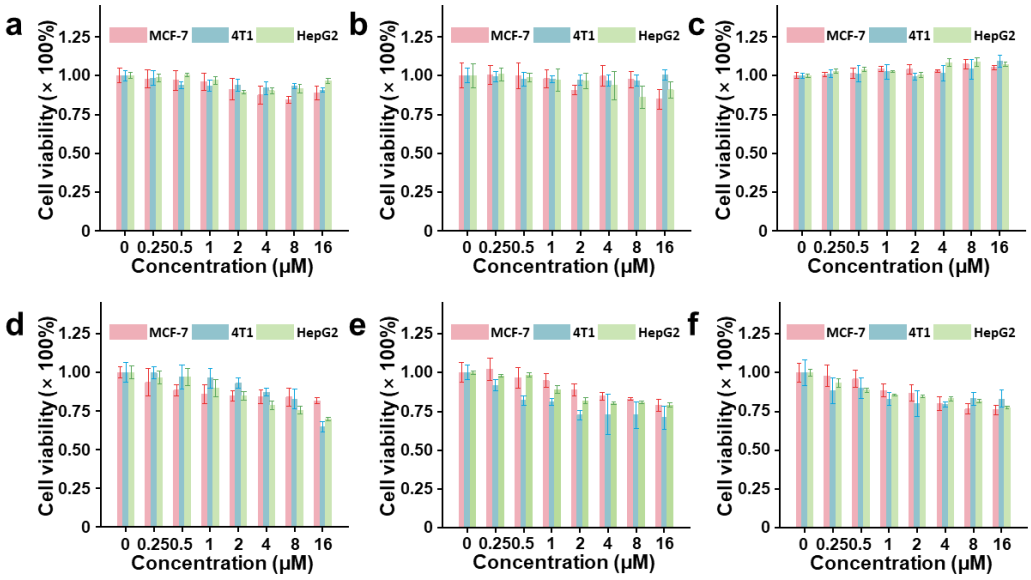

Supplementary Fig. 9 Cell viability of different cells (MCF-7, HepG2 and 4T1 cells) stained with different concentration of N1-N6 (a-f).

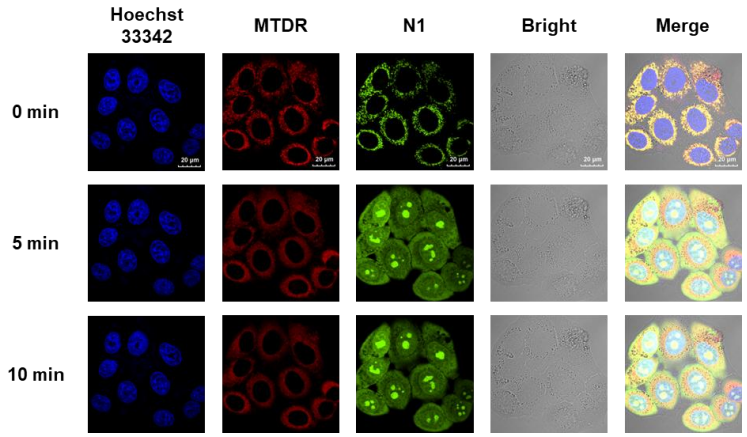

Supplementary Fig. 10 Confocal images of HepG2 cells stained with N1(2 μM), Hoechst 33342 and MTDR under light irradiation (the light is from the laser of confocal microscopy, 488 nm). N1: λ_{ex} = 488 nm, λ_{em} = 600–650 nm; Hoechst 33342: λ_{ex} = 405 nm, λ_{em} = 430–480 nm; MTDR: λ_{ex} = 640 nm, λ_{em} = 650–700 nm. Scale bar: 20 μm.

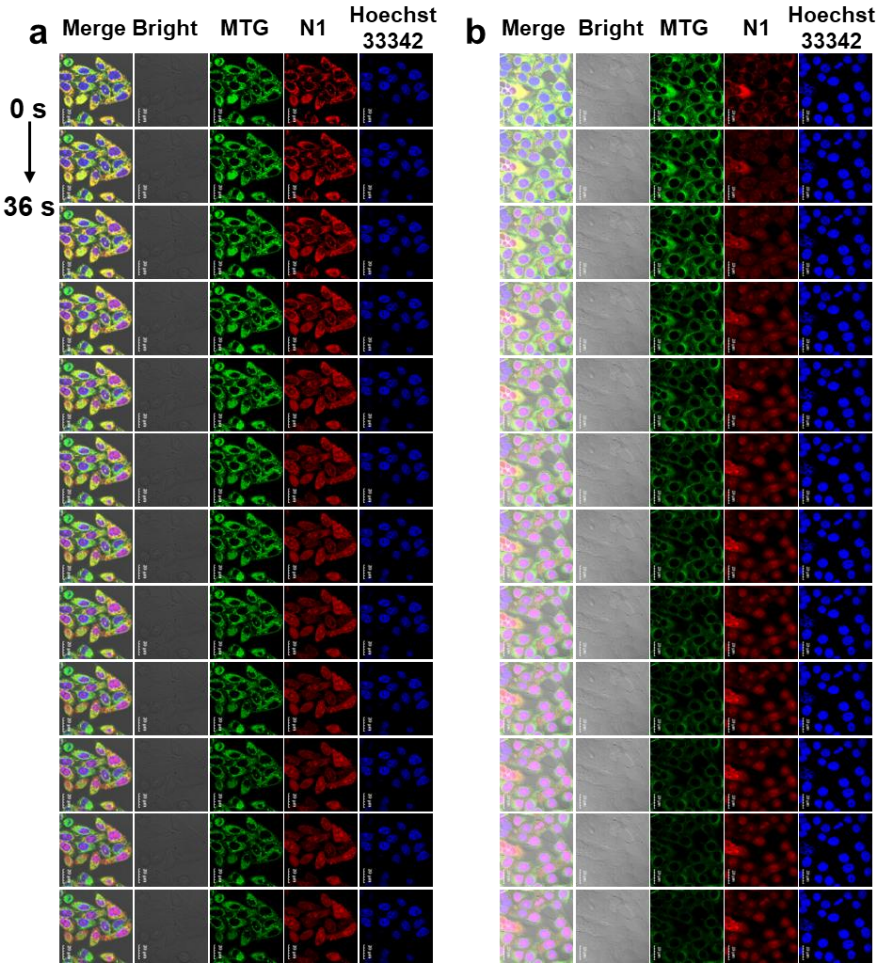

Supplementary Fig. 11 Fluorescent imaging of MCF-7 (a) and 4T1 cells (b) stained with N1 (2 μM) under light irradiation (collect images at 3 seconds intervals with continuous irradiation, the light is from the laser of confocal microscopy, 488 nm). N1: λ_{ex} = 488 nm, λ_{em} = 600–650 nm; Hoechst 33342: λ_{ex} = 405 nm, λ_{em} = 430–480 nm; MTG: λ_{ex} = 488 nm, λ_{em} = 500–550 nm. Scale bar: 20 μm.

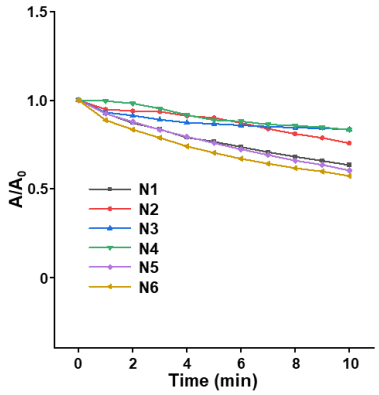

Supplementary Fig. 12 Decomposition rates of DPBF in the presence of N1-N6 under light irradiation (520 nm, 10 mW/cm^2), where A_0 and A refer to the maximum absorption of DPBF at 410 nm.

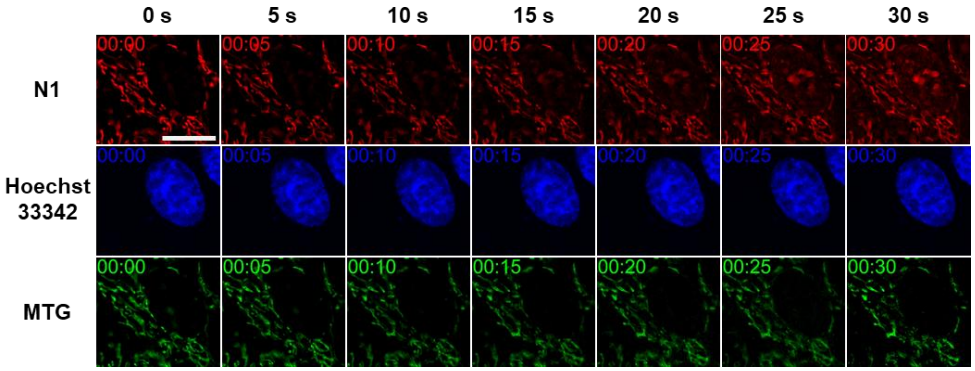

Supplementary Fig. 13 Super-resolution SIM images of HepG2 cells stained with N1 (2 μM), Hoechst 33342 and MTG under light irradiation (the light is from the laser of confocal microscopy, 488 nm). N1: λ_{ex} = 488 nm, λ_{em} = 600–650 nm; Hoechst 33342: λ_{ex} = 405 nm, λ_{em} = 430–480 nm; MTG: λ_{ex} = 488 nm, λ_{em} = 500–550 nm. Scale bar: 10 μm.

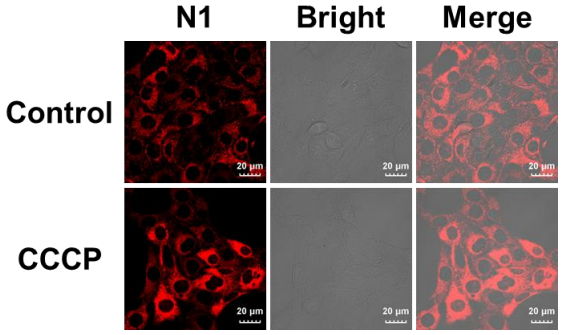

Supplementary Fig. 14 Fluorescent imaging of HepG2 cells stained at N1 (2 μM) with different mitochondrial membrane potentials. HepG2 cells were treated using CCCP (50 μM) for 30 minutes. N1: λ_{ex} = 488 nm, λ_{em} = 600–650 nm, Scale bar: 20 μm.

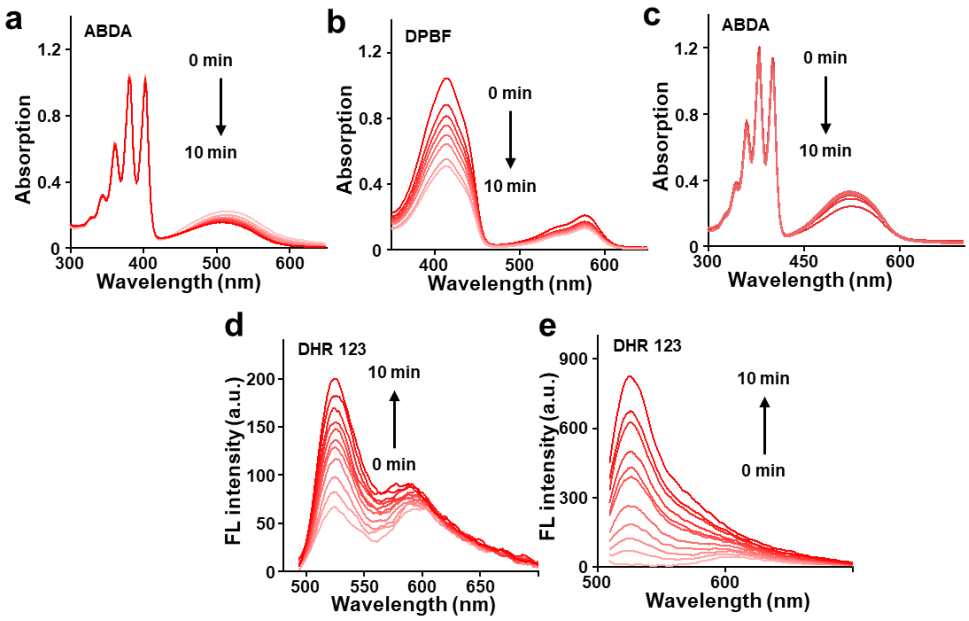

Supplementary Fig. 15 Absorption spectra of ABDA in the presence of N7 (a) and N9 (c) under light irradiation. (b) Absorption spectrum of DPBF in the presence of N8 under light irradiation. Emission spectra of DHR 123 in the presence of N8 (d) and N9 (e) under light irradiation. Condition of light irradiation of N7 and N9: 520 nm, 10 mW/cm^2; condition of light irradiation of N8: 540 nm, 10 mW/cm^2. DHR 123: λ_{ex} = 485 nm.

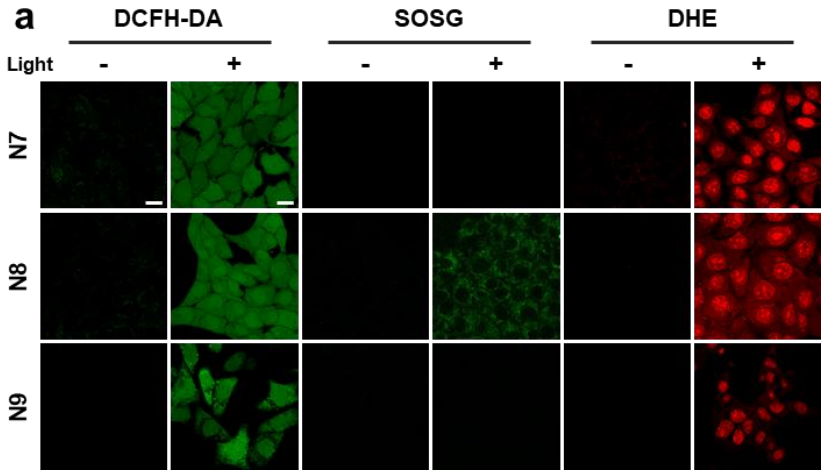

Supplementary Fig. 16 Fluorescent images of 4T1 cells stained using various ROS indicator (DCFH-DA, SOSG and DHE) and N7–N9 with or without light irradiation (520 nm, 10 mW/cm^2, 10 min). Scale bars: 20 μm.

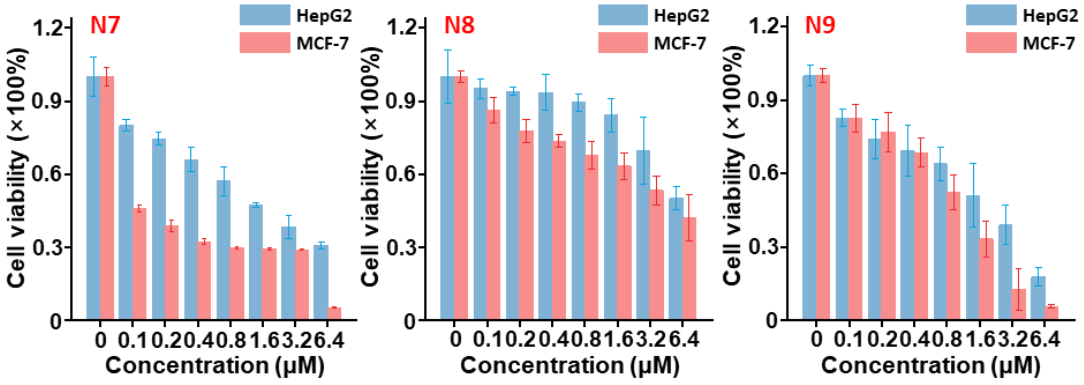

Supplementary Fig. 17 Cell viability of MCF-7 and HepG2 cells stained with N7–N9 under light irradiation (520 nm, 20 mW/cm^2, 10 min), n=3.

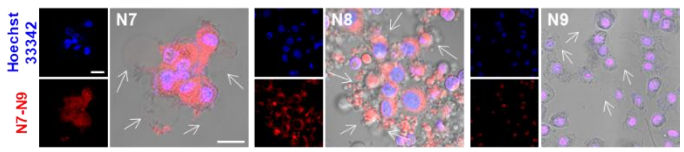

Supplementary Fig. 18 Fluorescent imaging of 4T1 cells co-stained with Hoechst 33342 and N7–N9 after light irradiation (520 nm, 10 mW/cm^2, 10 min). Scale bars:

20 μm.

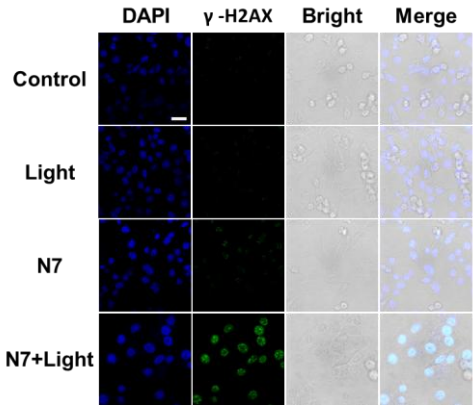

Supplementary Fig. 19 Immunofluorescence imaging of DNA damage induced by N7 (2 μM) in 4T1 cells. DAPI: λ_{ex} = 405 nm, λ_{em} = 440–550 nm. Scale bar: 20 μm.

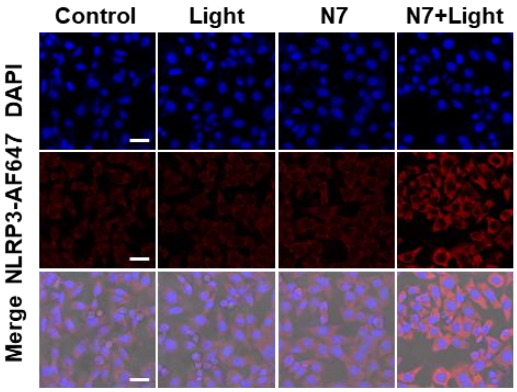

Supplementary Fig. 20 Immunofluorescence analysis of NLRP3 (secondary antibodies conjugated to Alexa Fluor-647 were used) expression in 4T1 cells treated with different conditions, combined with DAPI co-staining for nuclear localization. Scale bars: 20 μm.

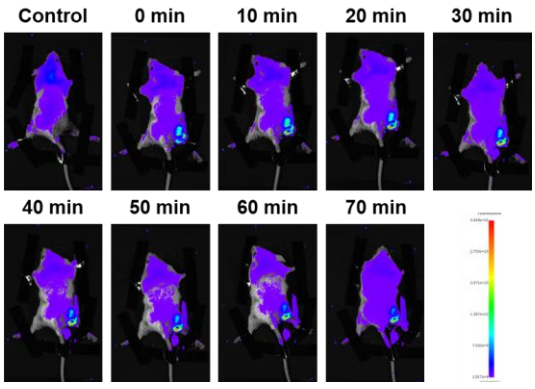

Supplementary Fig. 21 Fluorescent imaging of 4T1 cells bearing mice before and after intra-tumoral injection of N7 (4 μM, 100 μL).

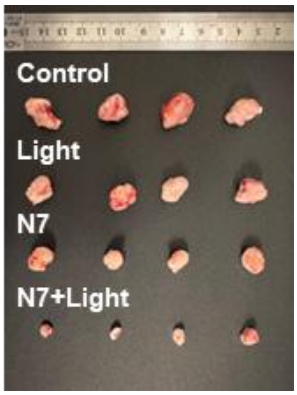

Supplementary Fig. 22 Photographs of excised tumors in different treatment groups on day 14.

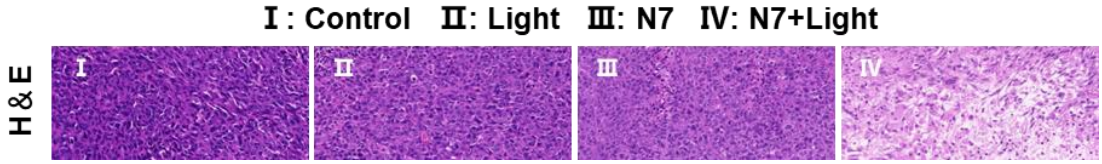

Supplementary Fig. 23 H&E staining of tumor tissue of different groups after treatments. Scale bar: 500 μm.

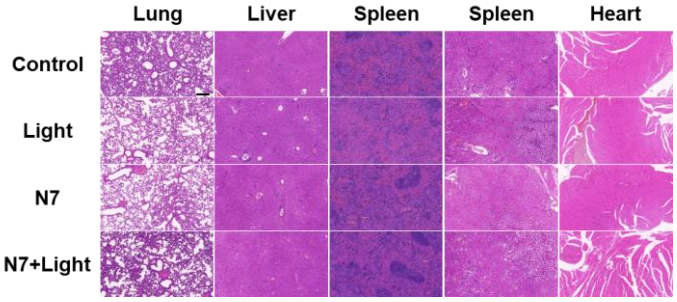

Supplementary Fig. 24 H&E staining of major organs of different groups after treatments. Scale bar: 500 μm.

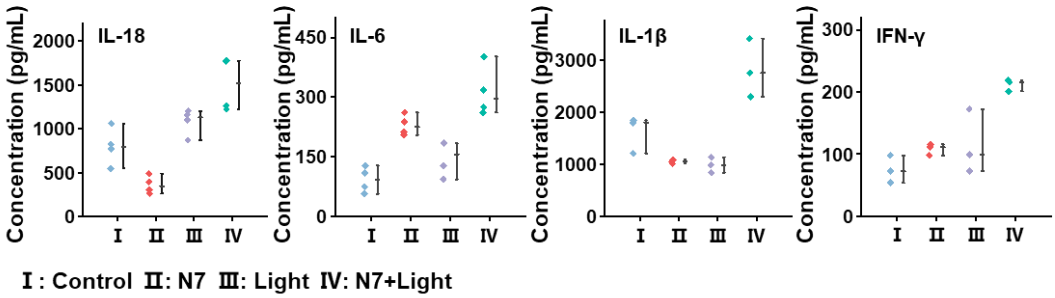

Supplementary Fig. 25 Elisa analysis of IL-6, IL-18, IL-1β and IFN-γ levels in tumor tissues after different treatments. Mean ± SD, n = 4.

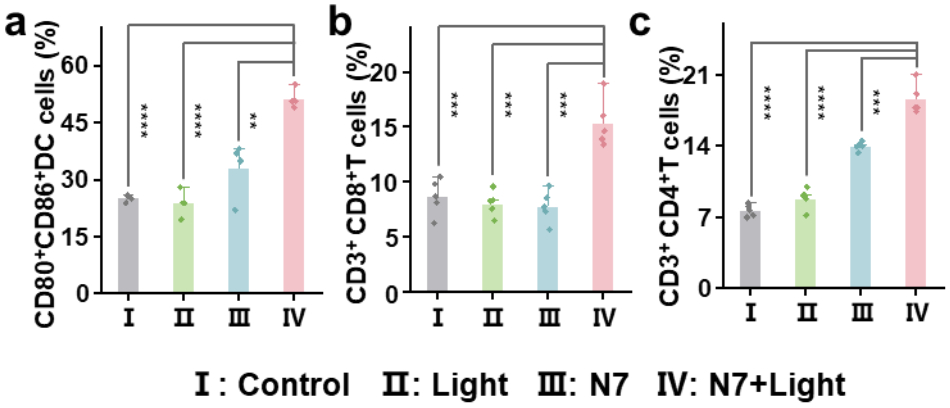

Supplementary Fig. 26 Statistical analysis of mature dendritic cells ($CD80^+CD86^+$ cells) in tumors (a), as well as cytotoxic T cells ($CD8^+$, $CD3^+$ cells) (b) and helper T cells ($CD4^+$, $CD3^+$ cells) (c) in tumors and spleens of mice in different treatment groups. Mean ± SD, n = 4.

3. Characterization of compounds

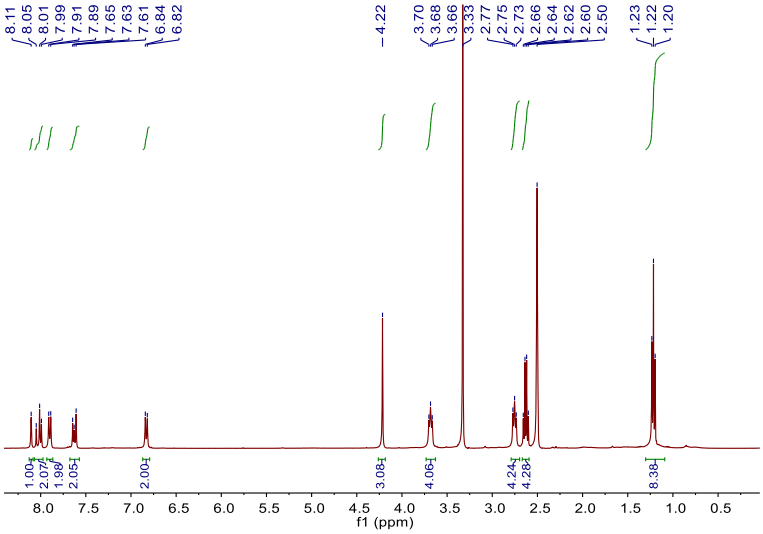

Supplementary Fig. 27 ^{1}H NMR spectrum of **N1** in DMSO-d_6.

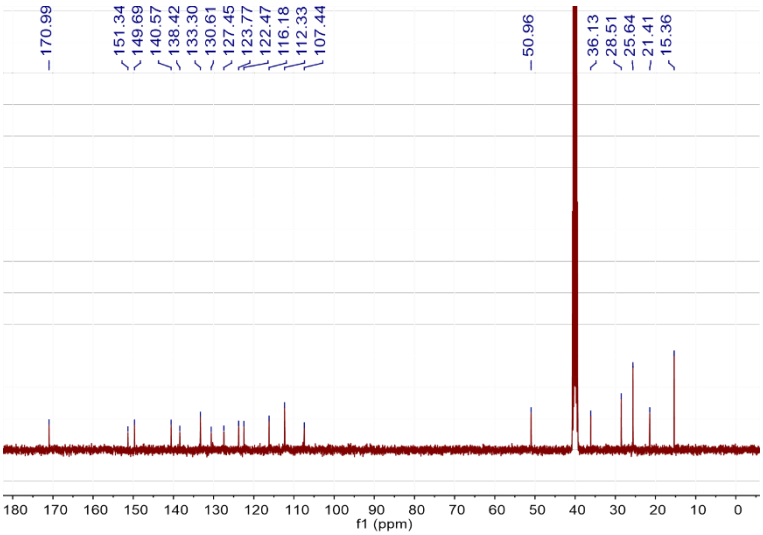

Supplementary Fig. 28 ^{13}C NMR spectrum of **N1** in DMSO-d_6.

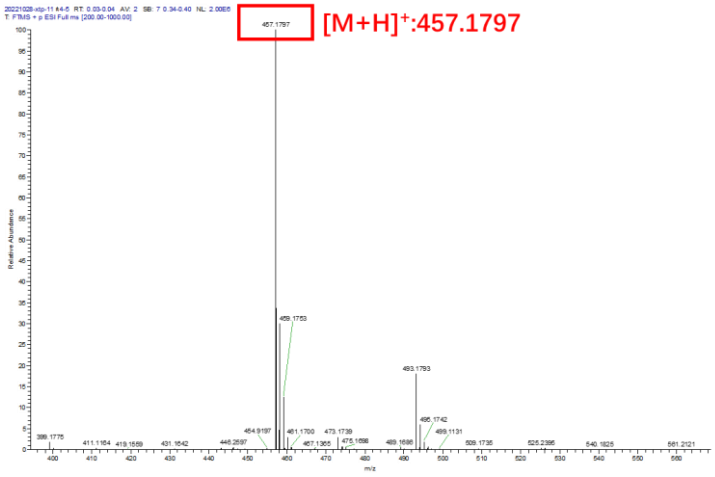

Supplementary Fig. 29 High resolution mass spectrum of **N1**.

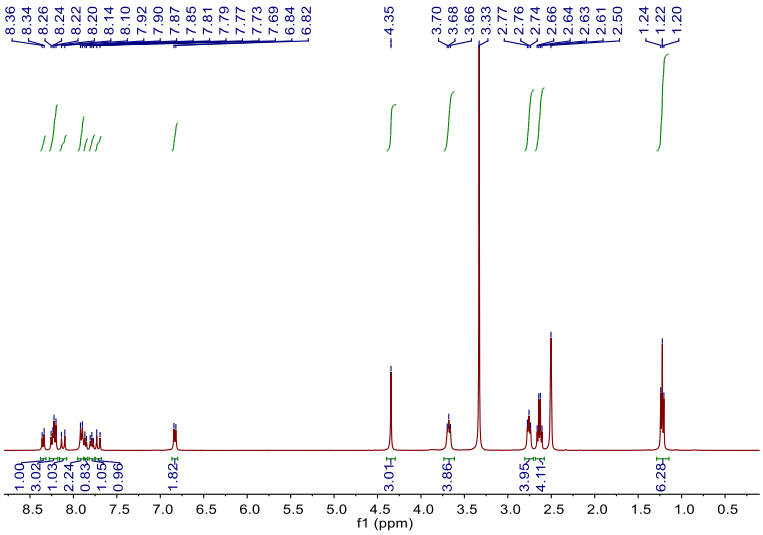

Supplementary Fig. 30 ^{1}H NMR spectrum of **N2** in DMSO-d_6.

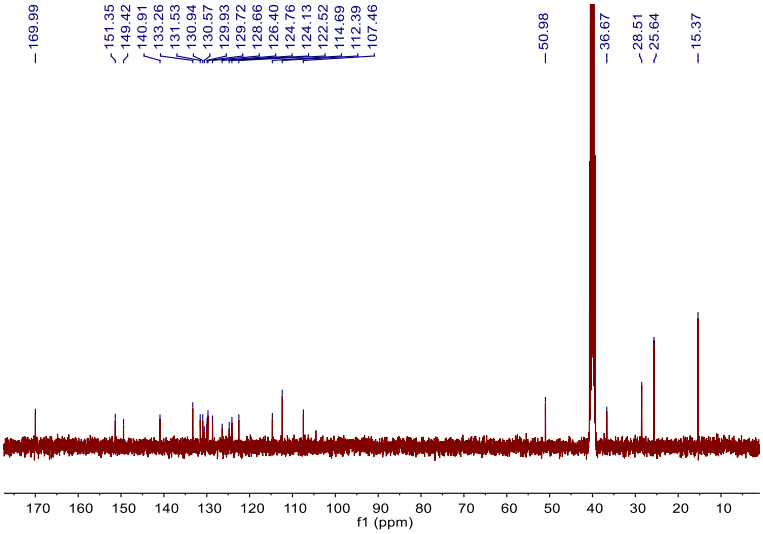

Supplementary Fig. 31 ^{13}C NMR spectrum of **N2** in DMSO-d_6.

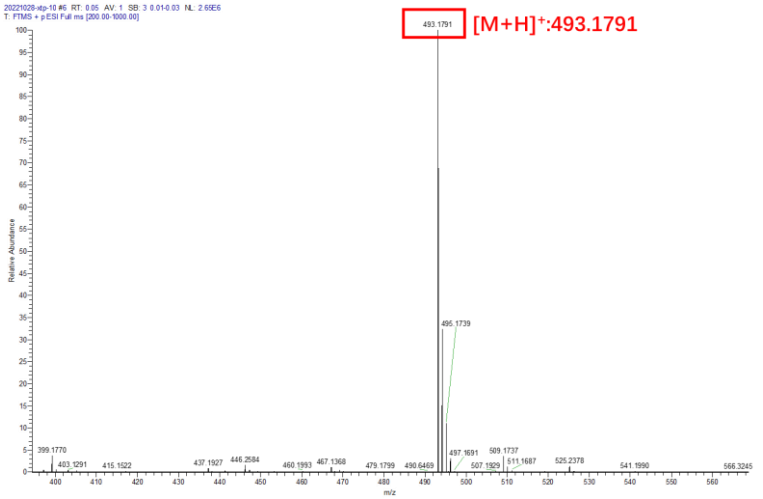

Supplementary Fig. 32 High resolution mass spectrum of **N2**.

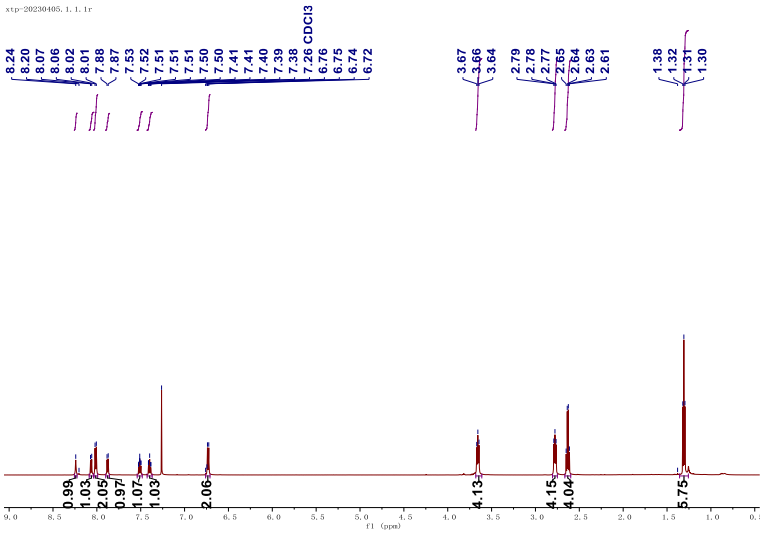

Supplementary Fig. 33 ^{1}H NMR spectrum of **N3** in $CDCl_3$-*d*.

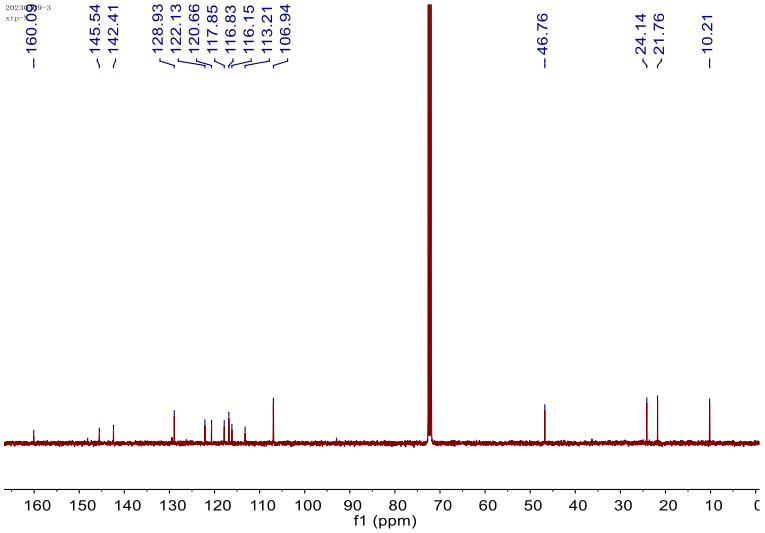

Supplementary Fig. 34 ^{13}C NMR spectrum of **N3** in DMSO-d_6.

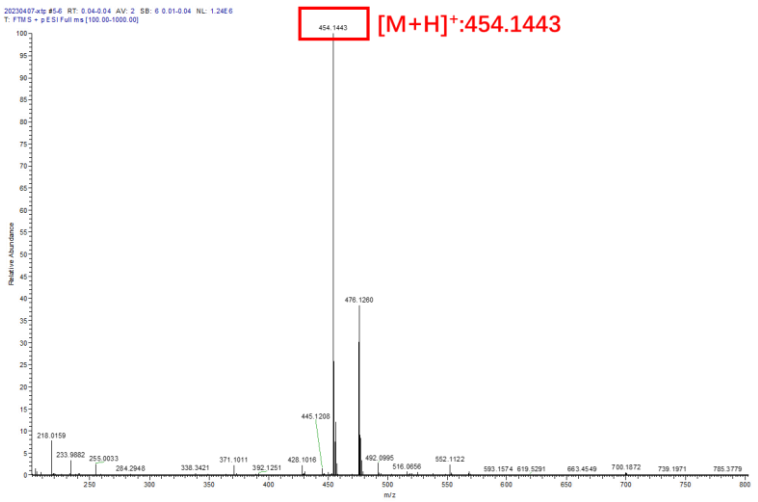

Supplementary Fig. 35 High resolution mass spectrum of **N3**.

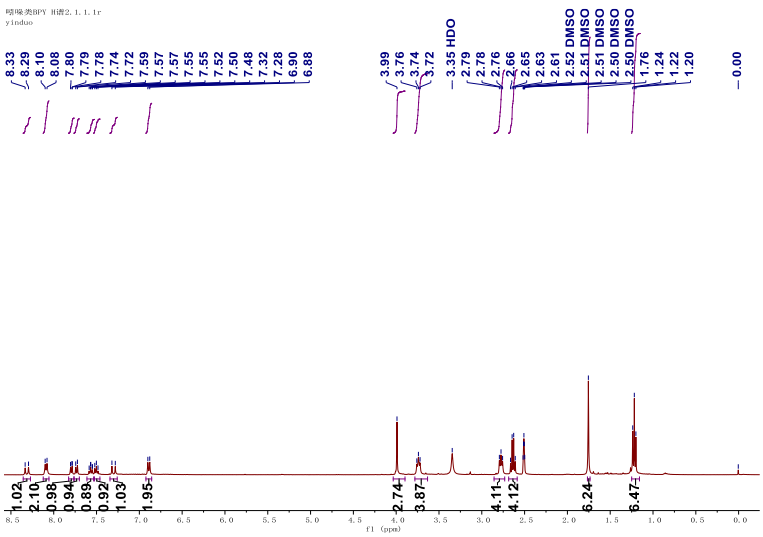

Supplementary Fig. 36 ^{1}H NMR spectrum of **N4** in DMSO-d_6.

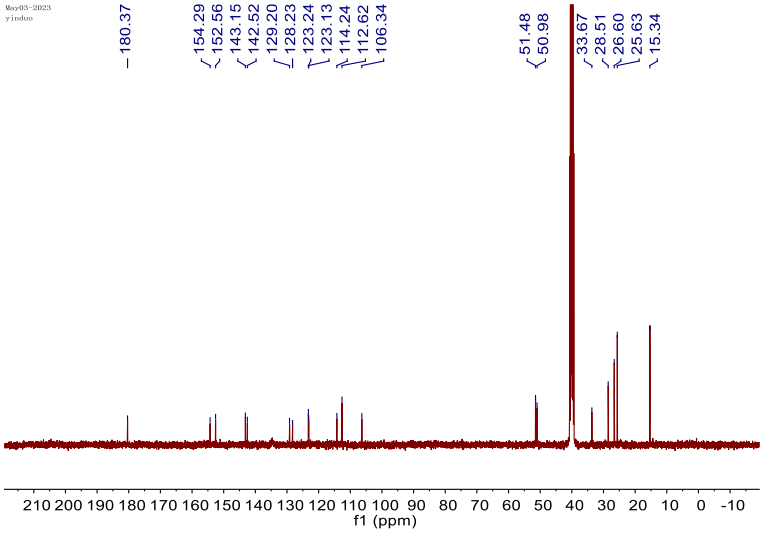

Supplementary Fig. 37 ^{13}C NMR spectrum of **N4** in DMSO-d_6.

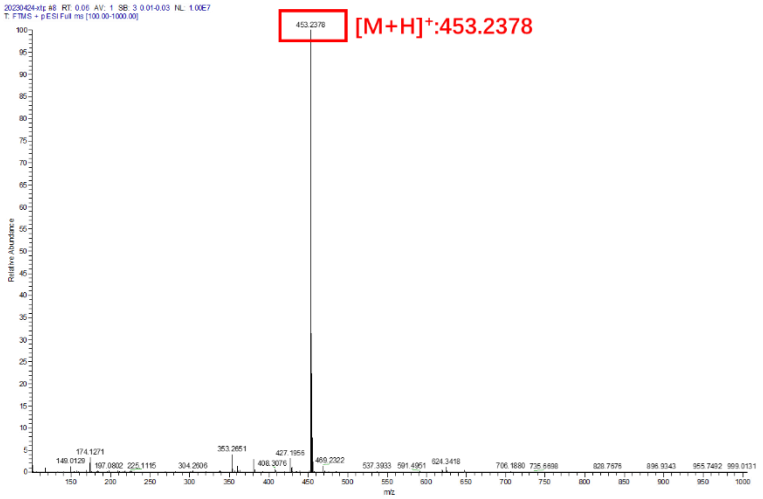

Supplementary Fig. 38 High resolution mass spectrum of **N4**.

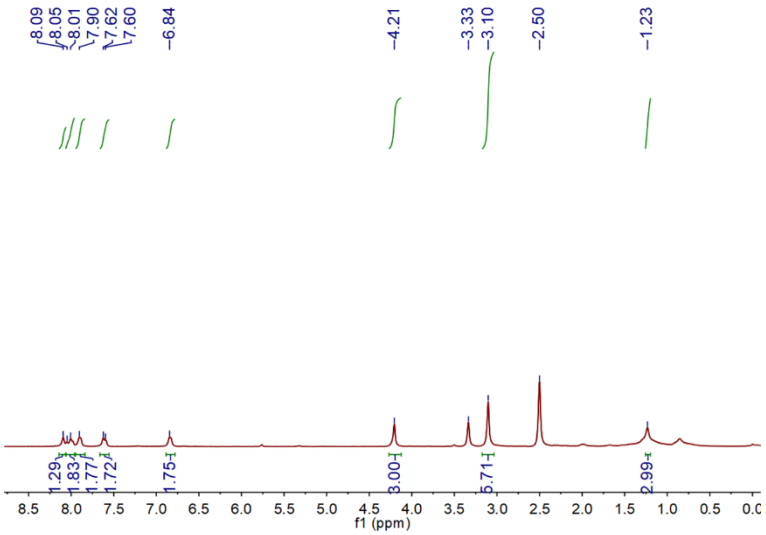

Supplementary Fig. 39 ^{1}H NMR spectrum of **N5** in DMSO-d_6.

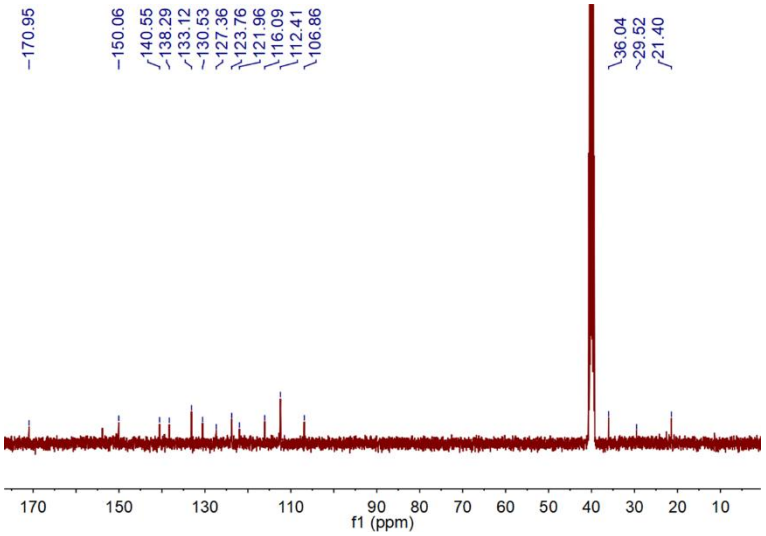

Supplementary Fig. 40 ^{13}C NMR spectrum of **N5** in DMSO-d_6.

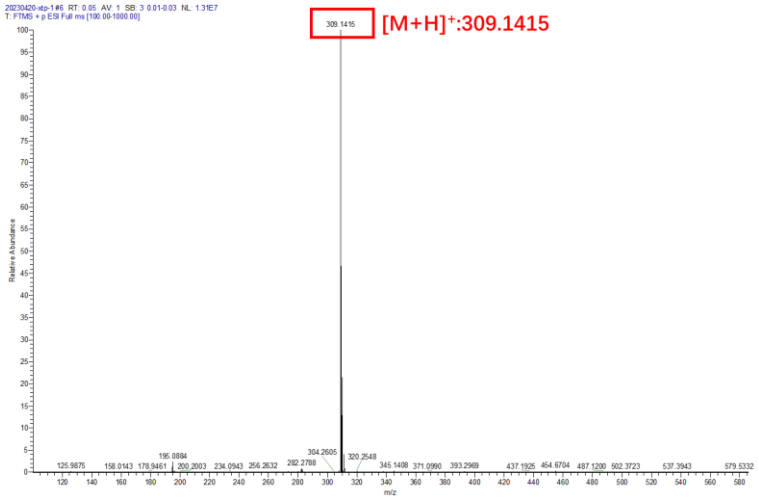

Supplementary Fig. 41 High resolution mass spectrum of **N5**.

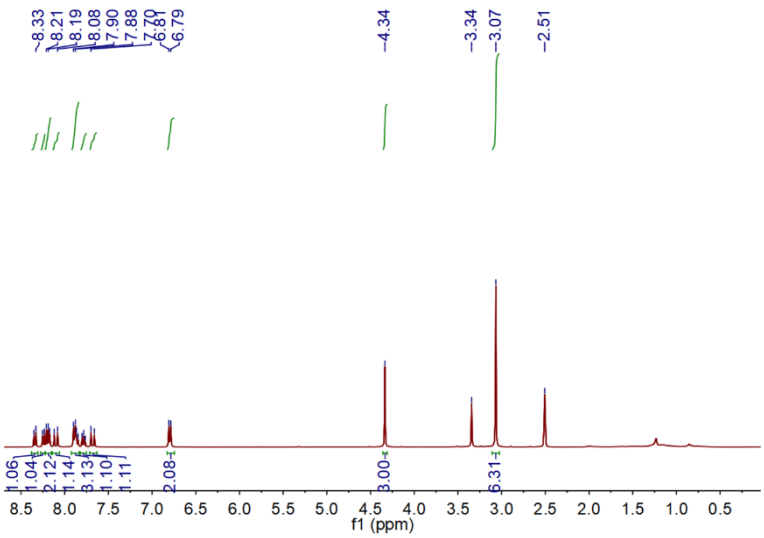

Supplementary Fig. 42 ^{1}H NMR spectrum of **N6** in DMSO-d_6.

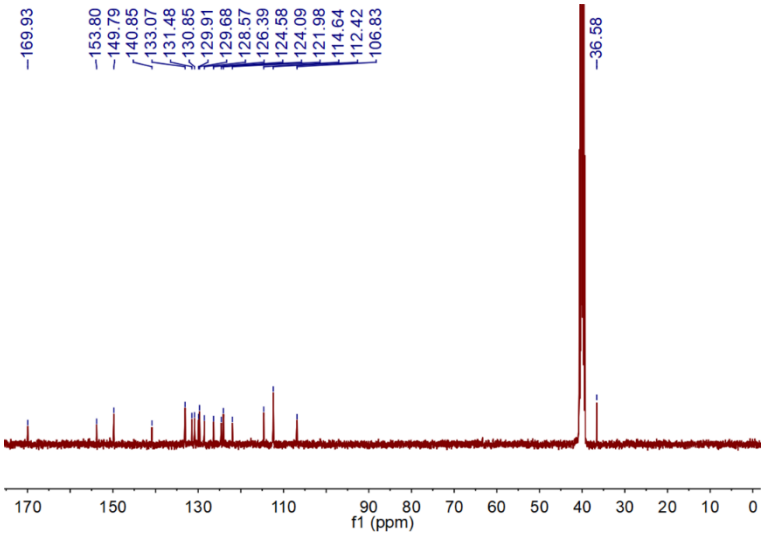

Supplementary Fig. 43 ^{13}C NMR spectrum of **N6** in DMSO-d_6.

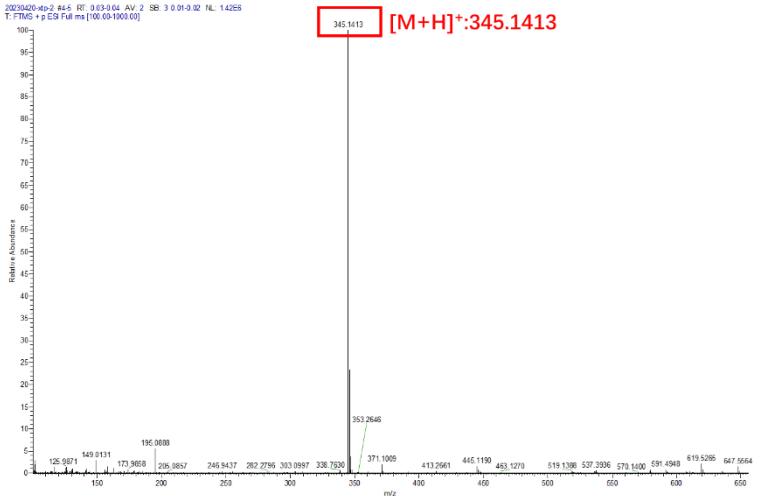

Supplementary Fig. 44 High resolution mass spectrum of **N6**.

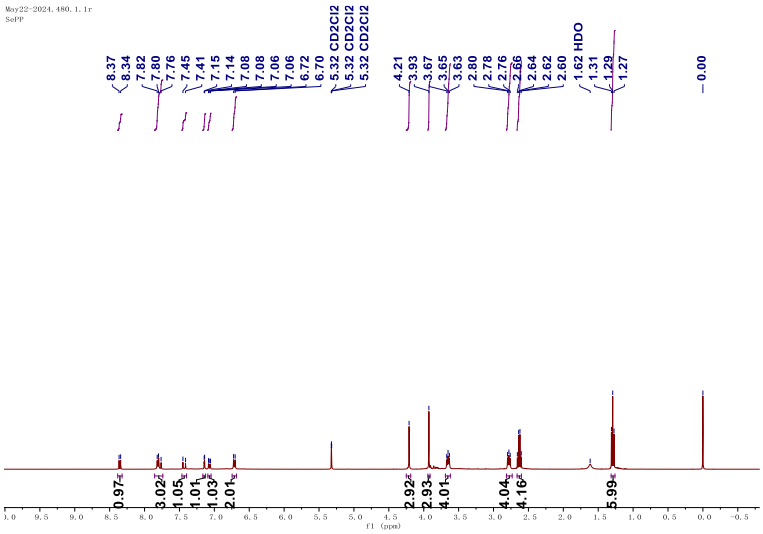

Supplementary Fig. 45 ^{1}H NMR spectrum of **N7** in CD_2Cl_2-d_2.

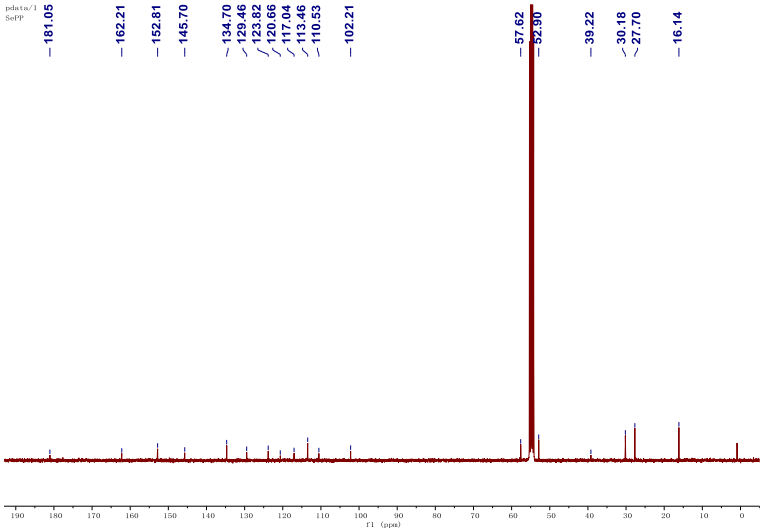

Supplementary Fig. 46 ^{13}C NMR spectrum of **N7** in CD_2Cl_2-d_2.

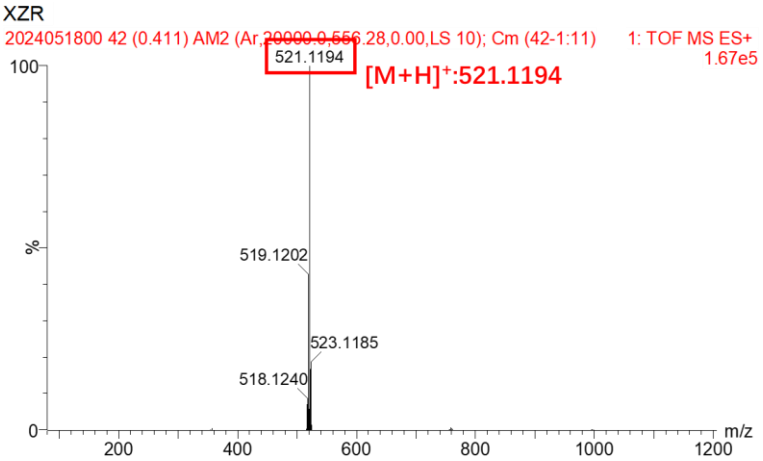

Supplementary Fig. 47 High resolution mass spectrum of **N7**.

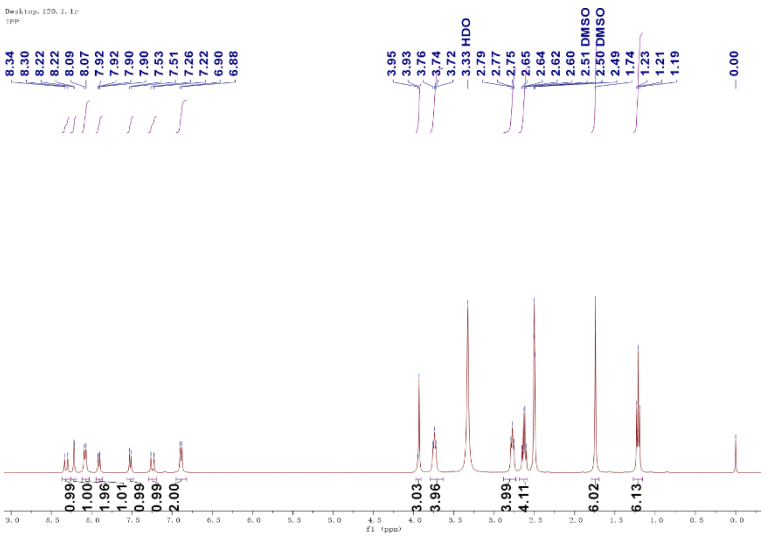

Supplementary Fig. 48 ^{1}H NMR spectrum of **N8** in DMSO-d_6.

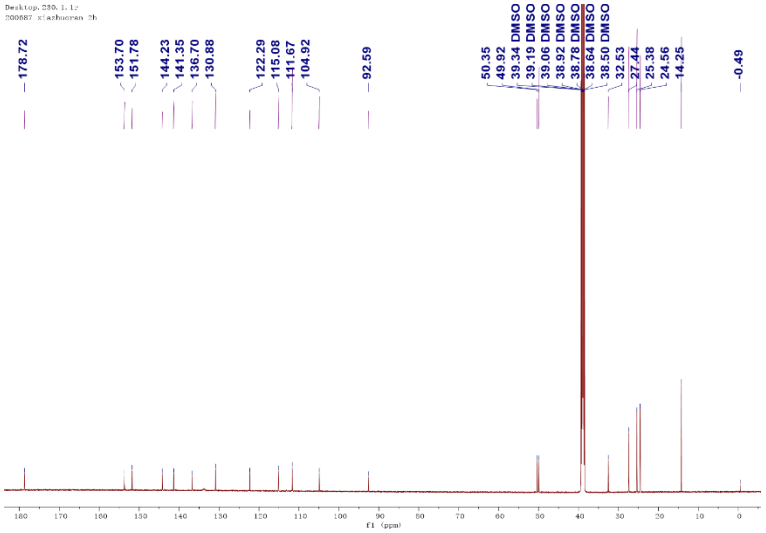

Supplementary Fig. 49 ^{13}C NMR spectrum of **N8** in DMSO-d_6.

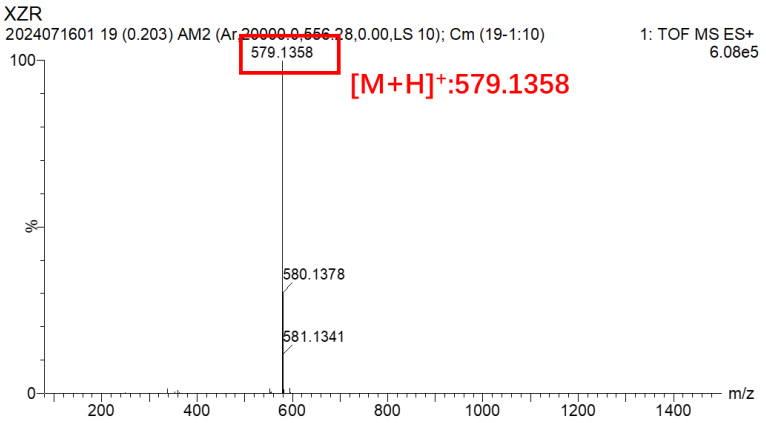

Supplementary Fig. 50 High resolution mass spectrum of **N8**.

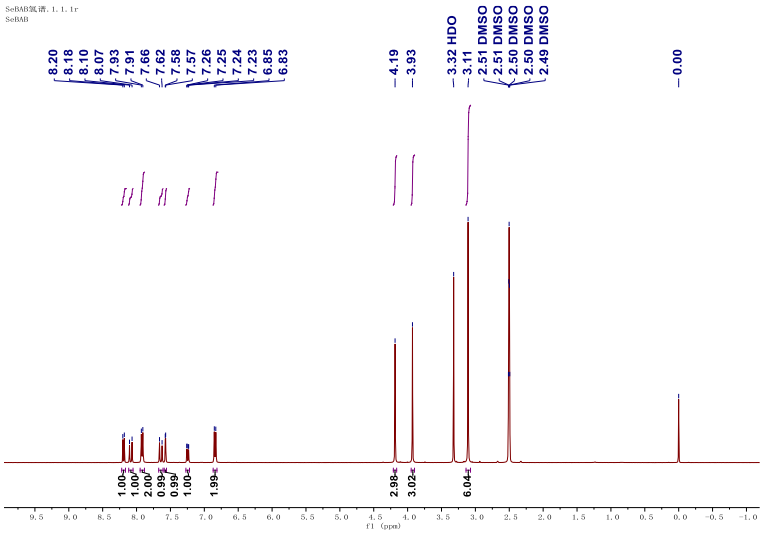

Supplementary Fig. 51 ^{1}H NMR spectrum of **N9** in DMSO-d_6.

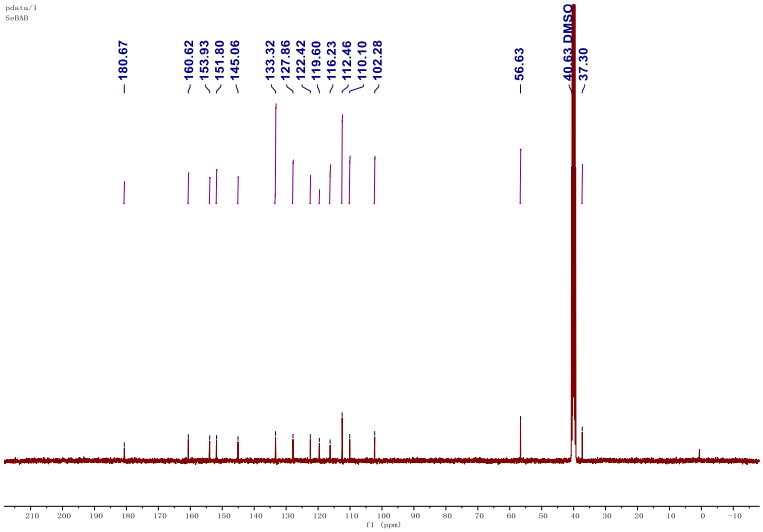

Supplementary Fig. 52 ^{13}C NMR spectrum of **N9** in DMSO-d_6.

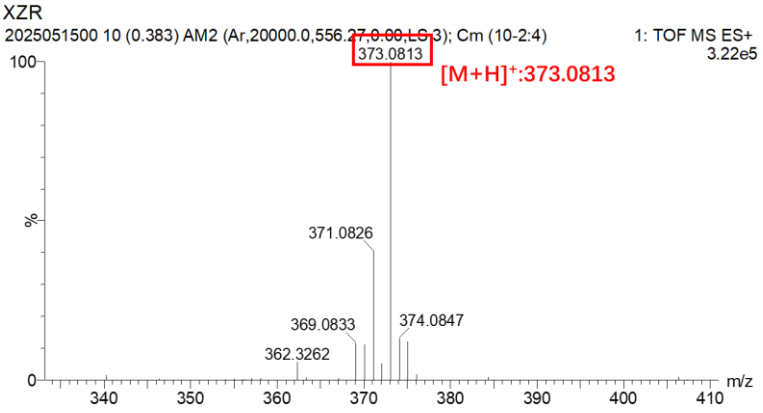

Supplementary Fig. 53 High resolution mass spectrum of **N9**.

5. References

[1] Gu, H. *et al.* Tuning exciton coupling of non-conjugated cyanine dimers for efffcient photodynamic immunotherapy. *J. Am. Chem. Soc.* 2025, **147**, 20778−20789.

[2] Ding, J. *et al.* A photoactivatable tumor-targeting in situ nanovaccine for large-volume tumor therapy. *Smart Mol.* 2025, **3**, e70014.

[3] Xia, T. *et al.* Nucleic acid probe-based difunctional hematology analysis kit for peripheral blood cell analysis. *ACS Sens.* 2022, **7**, 469−476.

[4] Xia, T. *et al.* mtDNA-triggered pH response signal-amplified fluorescent probe for multiple cell discrimination. *Chin. Chem. Lett.* **35**, 3, 2024, 108577, 1001-8417, https://doi.org/10.1016/j.cclet.2023.108577.

[5] Xia, T. *et al.* Light-driven mitochondrion-to-nucleus DNA cascade fluorescence imaging and enhanced cancer cell photoablation. *J. Am. Chem. Soc.* 2024, **146**, 12941−12949.